Check for updates

Article

JOURNAL OF ELASTOMERS & PLASTICS

Journal of Elastomers & Plastics
2017, Vol. 49(3) 209–225
© The Author(s) 2016
Reprints and permissions:
sagepub.co.uk/journalsPermissions.nav
DOI: 10.1177/0095244316644859
journals.sagepub.com/home/jep
SAGE

Mechanical properties and morphology of polypropylene/poly(acrylonitrile–butadiene–styrene) nanocomposites: Effect of compatibilizer and montmorillonite content

Mohamad Al Hafiz Ibrahim[1], Azman Hassan[1], Mat Uzir Wahit[2], Mahbub Hasan[3] and Munirah Mokhtar[1]

Abstract

Polypropylene (PP)/poly(acrylonitrile–butadiene–styrene) (ABS) blends containing montmorillonite (MMT) compatibilized with polypropylene-grafted maleic anhydride were prepared by melt extrusion using twin screw extruder followed by injection molding. Mechanical properties were evaluated through tensile, flexural, and impact testing. The microstructure and formation of nanocomposites were assessed by scanning and transmission electron microscopy and X-ray diffraction (XRD). Incorporation of polypropylene-grafted maleic anhydride and MMT into PP/ABS blend led to higher strength and stiffness but at the expense of toughness. Scanning electron micrographs revealed a fine and homogeneous dispersion of ABS phase in PP matrix. Both XRD and transmission electron microscopic analysis revealed the formation of intercalated clay silicate layer in PP/ABS nanocomposites.

Keywords

Mechanical properties, morphology, nanocomposites, blending, compatibilization

[1] Department of Polymer Engineering, Faculty of Chemical Engineering, Universiti Teknologi Malaysia (UTM), Johor, Malaysia
[2] Center for Composites, Universiti Teknologi Malaysia (UTM), Johor, Malaysia
[3] Department of Materials and Metallurgical Engineering, Bangladesh University of Engineering and Technology, Dhaka, Bangladesh

Corresponding author:
Azman Hassan, Department of Polymer Engineering, Faculty of Chemical Engineering, Universiti Teknologi Malaysia (UTM), 81310, Skudai, Johor, Malaysia.
Email: azmanh@cheme.utm.my

Introduction

Incorporation of nanofillers into polymer matrices is a popular strategy used to develop new materials with specific beneficial properties, and this method has attracted considerable interest as indicated by numerous publications.[1–4] These nanofillers may be halloysite nanotubes, carbon nanotubes, montmorillonite (MMT), inorganic particles, and so on. In particular, polymer/clay nanocomposites based on MMT are good examples because they allow polymer properties to be improved. These nanocomposites exhibit superior properties such as enhanced mechanical properties, reduced gas permeability, and improved flame retardancy and thermal stability. As a result, polymer/clay systems hold great promise for industrial applications due to their ability to display synergistically advanced properties with relatively small amounts of clay loading.[3] To further utilize the unique performance of these nanoparticles, numerous researches have incorporated clay into polypropylene (PP) matrix, one of the widely used nonpolar polyolefin thermoplastics.[2]

The reason behind blending PP with acrylonitrile–butadiene–styrene (ABS) is to combine the good process ability of PP with the high impact properties of ABS resin, eventually producing a polymer blend with improved properties. Unfortunately, blends of PP and ABS are immiscible throughout the whole range of compositions and exhibited low impact toughness as large butadiene particles formed during the melt blending process reducing interfacial adhesion.[5] PP nanocomposites are relatively difficult to produce because PP does not contain any polar groups in its backbone chain, hence homogenous dispersion of the polar hydroxyl groups of organoclay in nonpolar PP cannot be easily obtained.[1,2] On the other hand, by introducing a polar functional group into the system, which is reactive toward the polymer matrix to the clay surface, higher degrees of dispersion of the clay layers could be achieved, thereby improving the mechanical properties of the nanocomposites.[6] The polar functional group most commonly used in this method is maleic anhydride modified PP or PP-grafted maleic anhydride (PP-g-MA). It is believed that the polar character of anhydride causes an affinity for the silicate surface such that the maleated PP or PP-g-MA can serve as a compatibilizer between the matrix and the filler.

Important examples for commercially available reactively compatibilized blends are blends of PP and ABS. An earlier report on PP/ABS blends by Patel et al. showed that the introduction of PP-g-acrylic acid into PP/ABS blends resulted in considerable improvement in impact strength and tensile modulus due to the stiffening effect of ABS.[7] Kum et al. also found similar pattern applied to mechanical properties when PP-g-SAN was added as a compatibilizer.[8] In another work on PP/ABS blends, Lee et al. reported that the compatibility of the PP/ABS blends increased when PP-g-MA was added and the resultant mechanical properties were optimum at 3 phr of PP-g-MA.[5]

Considering the role of nanoclays in the enhancement of mechanical performances of polymers, it is expected that the addition of nanoclays into a PP/ABS blend system may further improve its mechanical and thermal properties. In this context, a recently published report on ABS/PP nanocomposites focused mainly on the study of morphology of ABS/clay nanocomposites blended with PP, its viscosity ratio, and dynamic mechanical

Table 1. Designations of materials and their compositions.

Designation	Composition	Parts
P60	PP/ABS	60/40
P60G4	PP/ABS/PP-g-MA	60/40/4 phr
P60M3	PP/ABS/MMT	60/40/3 phr
P60M5	PP/ABS/MMT	60/40/5 phr
P60M3G4	PP/ABS/MMT/PP-g-MA	60/40/3 phr/4 phr
P60M5G4	PP/ABS/MMT/PP-g-MA	60/40/5 phr/4 phr

PP: polypropylene; PP-g-MA: polypropylene-grafted maleic anhydride; ABS: acrylonitrile–butadiene–styrene; MMT: montmorillonite.

properties. Sung et al. found that most of the clay existed in ABS continuous phase because of the affinity between the ABS and clay. They also discovered that the viscosity ratios decreased with increase in clay.[9]

Numerous studies on compatibilized PP/clay nanocomposites have been conducted including studies on the PP/PP-g-MA/clay which focused on the mechanical, morphological, and rheological properties; optical transmittance and mechanical properties of PP/PP-g-MA/clay; different types of compatibilizer on PP/clay; and recently, the mechanical and fracture behaviors of PP/PP-g-MA/clay.[3,10–12] Improvements are shown so far in most of the cases including mechanical and thermal properties.

Although numerous studies concerning the effect of compatibilizers on PP nanocomposites have been reported, the purpose of this study is to better understand the influence of compatibilizer and filler content on the structure–property relationship of polymer blend. The focus will be on the changes occurring in mechanical properties and morphology of compatibilized PP/ABS nanocomposites due to the incorporation of PP-g-MA.

Experimental

Materials

Homopolymer PP was supplied by Titan Petchem (M) Sdn. Bhd (Malaysia) under the trade name Titanpro 6331 (density = 0.91 g cm^{-3}, MFR (Mass Flow Rate) = 14 g/10 min (230°C/10 kg)). Commercial poly-ABS, Toyolac 100 322, was obtained from Toray Plastics (Malaysia) Sdn. Bhd (density = 1.04 g cm^{-3}, MFR = 15 g/10 min (220°C/10 kg)). PP-g-MA was purchased from ExxonMobil Chemicals (ExxonMobil Chemical Asia Pacific, Harbour Front Tower One, Singapore) under the trade name of Exxelor PO 1020 (density = 0.9 g cm^{-3}, MFR = 110 g/10 min (190°C/1.2 kg), MA graft level = 0.5–1.0 wt%). The clay or MMT used in this study was Nanomer 1.44P (Nanocor Inc., Hoffman Estates, Illinois, USA). The MMT was organically modified with octadecylamine.

Preparation of PP/ABS blend and nanocomposites

Blends of PP, ABS, PP-g-MA, and MMT were prepared according to Table 1. Nanocomposites were produced by melt compounding using a Berstoff (Hannover, Germany)

corotating twin screw extruder, with a barrel temperature of 180°C at the feed section, increasing to 220°C at the die head. The screw rotation speed was fixed at 50 r min^{-1}. Extruded nanocomposites pellets were dried and then injection molded into standard tensile, flexural, and Izod impact bars in a JSW (Muroran, Japan) Model NIOOB II 100 Ton Injection Molding machine using a barrel temperature of 180°C (feed) to 240°C (Nozzle), injection time of 10 s, and cooling time of 90 s. All samples were desiccated for about 24 h prior to testing.

Characterization techniques

Tensile and flexural tests were carried out according to ASTM D638-10 and ASTM D790-10 standards, using an Instron Model 4301 universal testing machine under ambient conditions. Crosshead speeds of 50 mm min^{-1} and 3 mm min^{-1} were used for tensile and flexural testing, respectively. The Izod impact test was performed in accordance to ASTM D256-10 standard on notched impact specimens using a Toyoseiki (Tokyo, Japan) impact tester with the capacity of 11 J and the weight of pendulum of 31.90 N. The purpose of notching the sample is to provide a stress concentration area that promotes a brittle rather than ductile failure. Five specimens of each formulation were tested and the average values are reported. The morphology of the room temperature fractured surface etched with tetrahydofuran (THF), 24 h, for ABS extraction was characterized with scanning electron microscopy (SEM) machine (Philips XL 40, Philips, Michigan, USA) after gold coatings. The coating equipment used is Model Bio-Rad Cool Sputter Coater (Bio-Rad, Singapore). XRD analysis was carried out on a Siemens (Berlin, Germany) D5000 X-ray diffractometer in order to confirm whether the PP/ABS/PP-g-MA/MMT nanocomposites had been formed. The diffraction patterns were recorded with a step size of 0.02°, from $2\theta = 2$ to 10°. The interlayer distances of the MMT in the nanocomposites were derived from the peak position (d_{001} reflections) in the XRD scans. The images of the microstructure of the PP/ABS nanocomposites were obtained using a Philips (CM12) transmission electron microscope with the accelerating voltage of 120 kV. The samples were microtomed by using an RMC Boeckeler Powertome machine (RMC Boeckeler, San Diego, USA). The thickness of the ultrathin samples was less than 100 nm. Samples were stained with uranyl acetate prior to the viewing process in TEM.

Results and discussion

Mechanical properties

Figure 1 shows that the incorporation of PP-g-MA has improved the tensile and flexural strength of PP/ABS blend and its nanocomposites. It can be seen that addition of 4 phr PP-g-MA to the PP/ABS blend caused a substantial improvement in the tensile and flexural strength of about 16% and 14%, respectively, while the increment were 15% and 9% for its nanocomposites. Similarly PP-g-MA also improved the tensile and flexural modulus of PP/ABS blend and nanocomposites as shown in Figure 2. Increases of as much as 6% and 13%, respectively, for the nanocomposites containing 5 phr of MMT were observed. Figures 1 and 2 also show the effect of MMT content on both strength and modulus (tensile

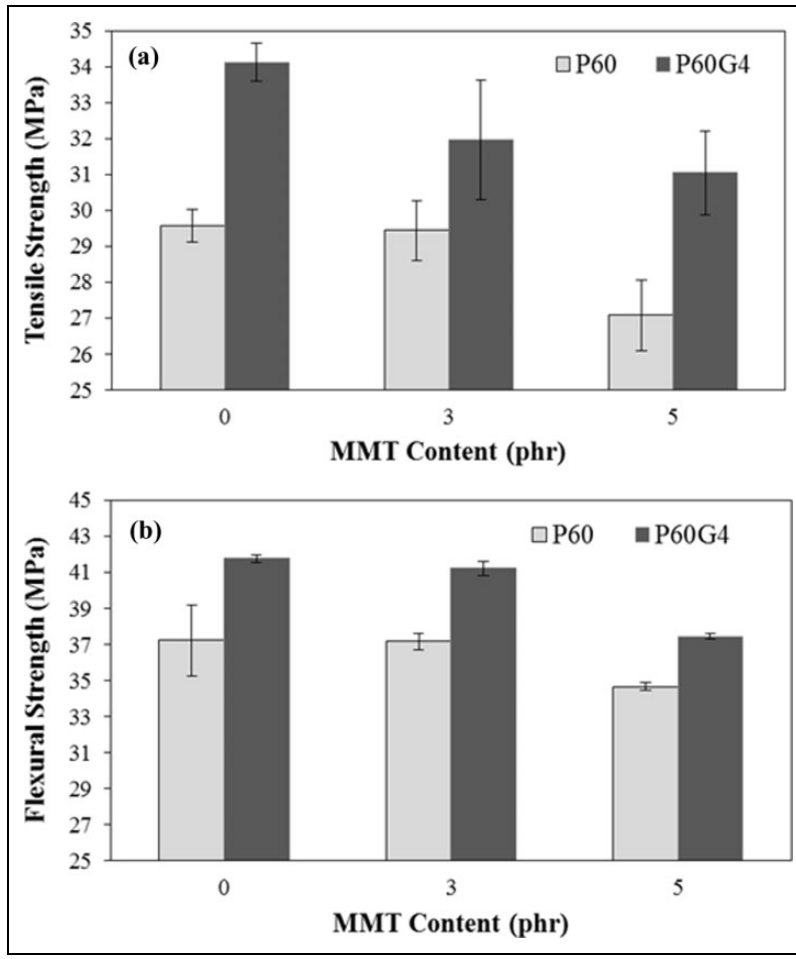

Figure 1. Effect of PP-g-MA and MMT content on (a) tensile strength and (b) flexural strength of PP/ABS blend and nanocomposites. PP-g-MA: polypropylene-grafted maleic anhydride; PP: polypropylene; ABS: acrylonitrile–butadiene–styrene; MMT: montmorillonite.

and flexural) of PP/ABS blend and its nanocomposites. The addition of 3 and 5 phr MMT increased the modulus of PP/ABS blend and nanocomposites significantly, however, the tensile and flexural strength showed slight decrease in values. These findings are in line with previous studies, which found similar enhancement in terms of stiffness upon incorporation of MMT.[4,6,11,13] As reported by Ding et al., the flexural modulus of PP nanocomposites increased remarkably with MMT content.[13] On that basis, the flexural modulus of PP/MMT nanocomposites with 6 phr MMT increased to 2.41 GPa compared to 1.27 GPa for neat PP. In a study conducted by Lai et al., it was found that the corresponding value for tensile modulus of PP nanocomposites increased by 6% from tensile

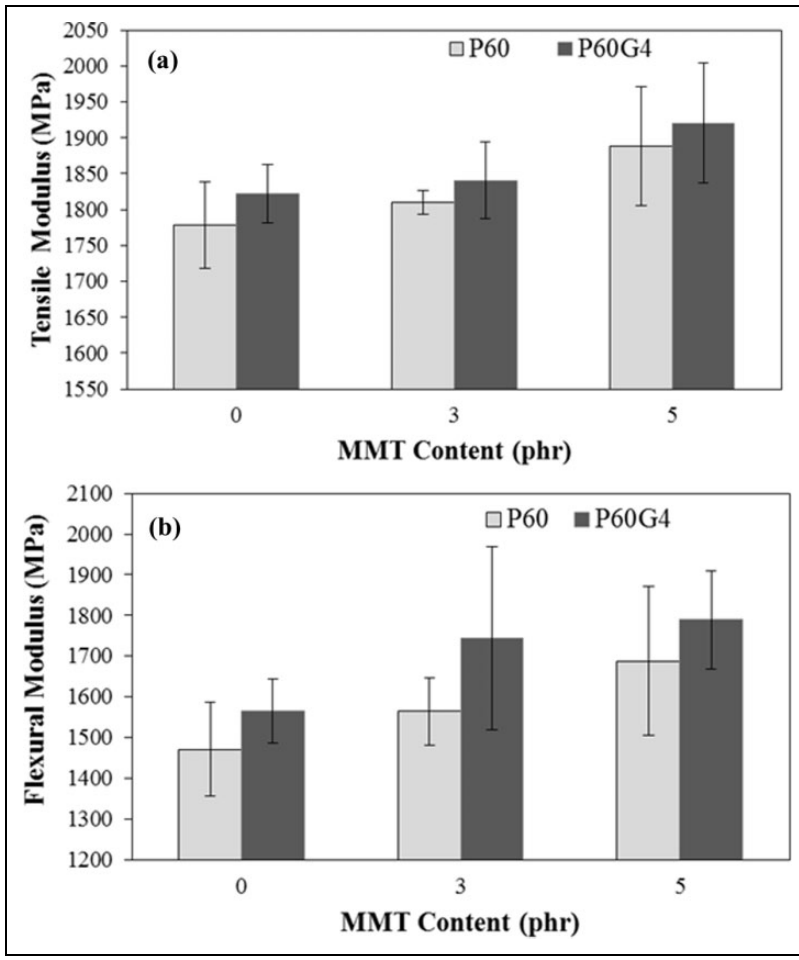

Figure 2. Effect of PP-g-MA and MMT content on (a) tensile modulus and (b) flexural modulus of PP/ABS blend and nanocomposites. PP-g-MA: polypropylene-grafted maleic anhydride; PP: polypropylene; ABS: acrylonitrile–butadiene–styrene; MMT: montmorillonite.

modulus of pristine PP.[11] From Figure 3, it is apparent that compatibilized compounds exhibit rather poor impact resistance. PP-g-MA does not show a positive effect on the impact strength of PP/ABS blend. A reduction of 50% was observed for compatibilized blend. As for nanocomposites, the use of PP-g-MA reduced the impact strength by about 9% and 3% for nanocomposites containing 3 and 5 phr MMT, respectively.

The improvement in tensile and flexural strength of PP/ABS blend upon addition of PP-g-MA can be attributed to the use of the compatibilizer, which reduced the interfacial tension between PP and ABS, subsequently allowing ABS to contribute strength much more effectively than in uncompatibilized blends. A decrease in interfacial tension

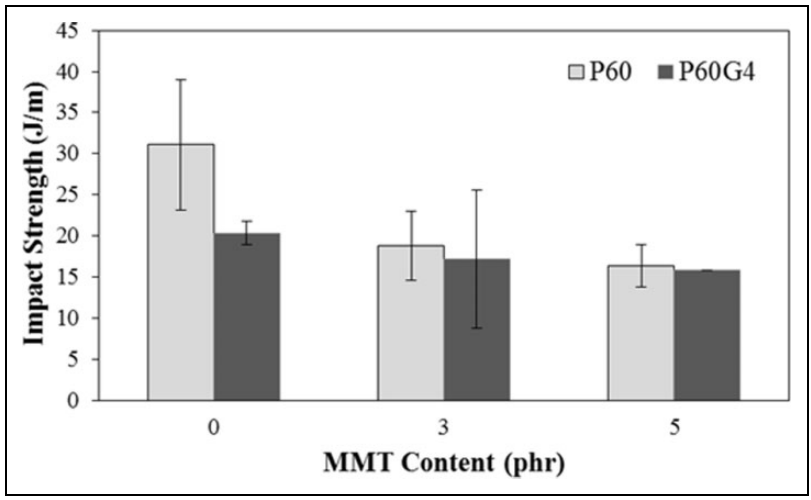

Figure 3. Effect of PP-g-MA and MMT content on Izod impact strength of PP/ABS blend and nanocomposites. PP-g-MA: polypropylene-grafted maleic anhydride; PP: polypropylene; ABS: acrylonitrile–butadiene–styrene; MMT: montmorillonite.

indicates that the compatibility between those polymers increased. This behavior is observed in a later SEM image in which the particle size of ABS decreased upon the addition of PP-g-MA. The decrease in particle size suggests the improvement in compatibility between PP and ABS, since the decrease of the particle size in polymer blends is related to the improvement of interfacial adhesion between two polymers.[5,14] This phenomenon is explained later in morphological part (SEM). As in nanocomposites, the improvement in strength is believed to be due to the ability of PP-g-MA to interact with the functionality of the MMT, promoting a chemical link between MMT and PP/ABS matrix. Similar findings were also reported by Lai et al., Kim et al., and Lim et al.[11,15,16]. According to Lai et al., the PP-g-MA compatibilized system conferred higher tensile strength than an uncompatibilized system. Hence, it is believed that interfacial phase and matrix properties are major factors in attaining the best performance of nanocomposites in terms of tensile properties. In addition, Kim et al. believed that the tensile and flexural strength of PP-g-MA-treated composites were significantly greater than those of the PP-g-MA nontreated composites due to the enhanced interfacial adhesion of the composites by PP-g-MA.[17]

The improvement in stiffness may be attributed to the formation of ABS-g-PP copolymer, which improved the interfacial adhesion between PP and ABS in the presence of PP-g-MA. The interaction between ABS and PP-g-MA, which resulted in ABS-g-PP, consequently formed hydrogen bonding between the anhydride group of PP-g-MA and the octadecylamine group of clay, when clay was intercalated into PP/ABS matrix. Kim et al. discovered that PP-g-MA was needed to achieve a better dispersion of the silicate platelets in a PP matrix and as a consequence, improved stiffness of PP nanocomposites.[15] Kim et al. produced similar findings, which revealed that the addition of

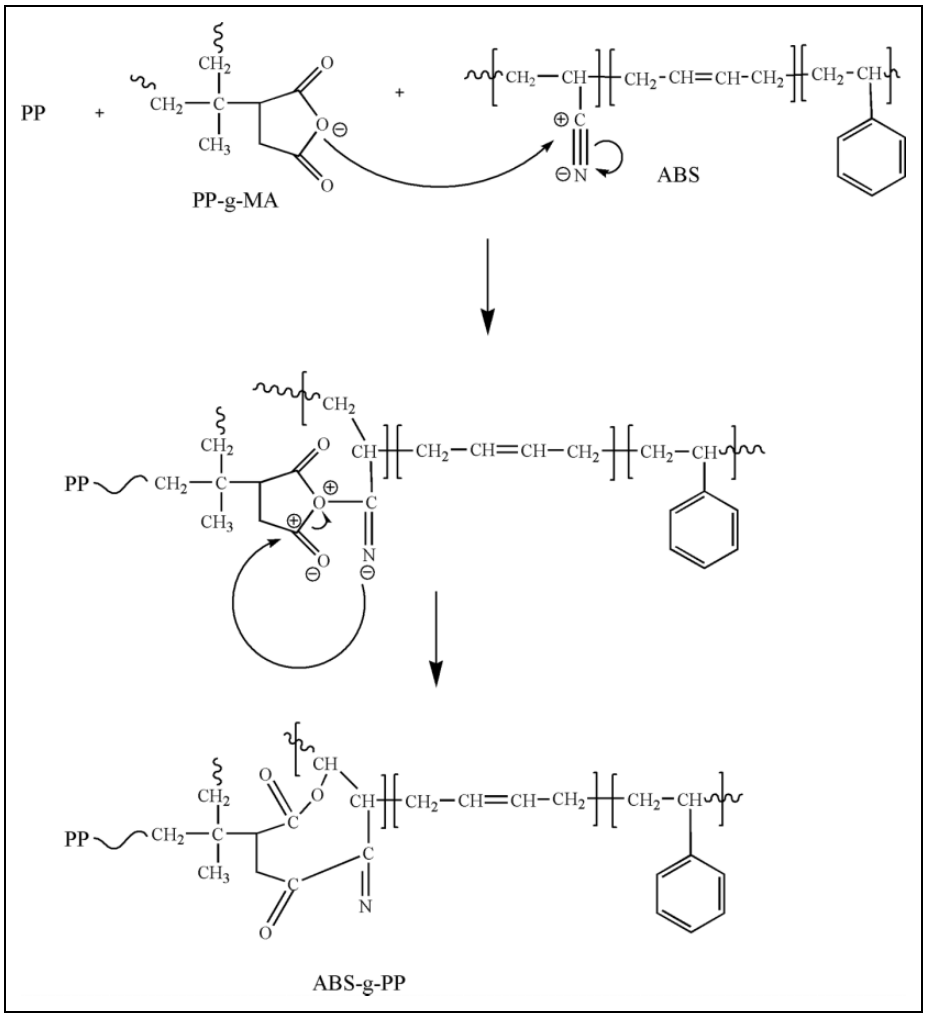

Figure 4. Possible chemical reaction between PP, ABS, and PP-g-MA. PP: polypropylene; ABS: acrylonitrile–butadiene–styrene; PP-g-MA: polypropylene-grafted maleic anhydride.

PP-g-MA on PP/MMT nanocomposites produced a significant increase in stiffness.[10] The possible interaction mechanism between PP, ABS, and PP-g-MA to form ABS-g-PP is proposed in Figure 4, while the interaction between MMT and the ABS-g-PP copolymer formed in the presence of PP-g-MA in PP/ABS blends is proposed in Figure 5.

The improvement in stiffness can also be caused by the reinforcing effect of fillers. Generally, several factors usually contribute to the reinforcement effect with respect to the clay, which are the rigid structure of clay, aspect ratio of platelet structure, degree of exfoliation, and the affinity with the matrix polymer.[18] The rigid structure of MMT,

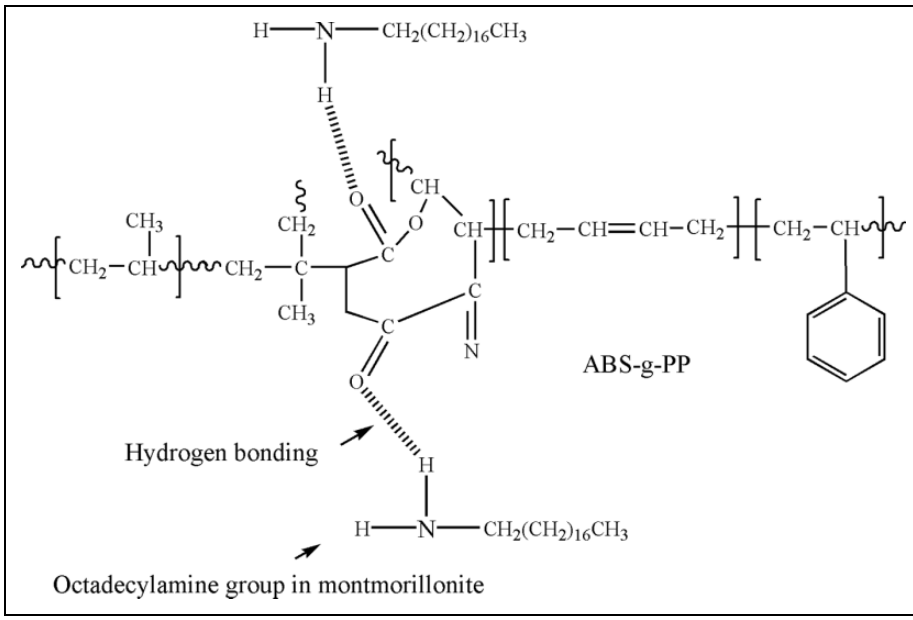

Figure 5. Chemical bonding between ABS-g-PP and MMT. PP: polypropylene; ABS: acrylonitrile–butadiene–styrene; MMT: montmorillonite.

which consists of silicate layers, constrains the molecular motion of PP and ABS chains, thus resulting in an increase in stiffness.[19] In general, the rigid structure of the fillers, which are strong and stiff, should be able to bear the stress applied to the system while the polymer, which is of low strength, should effectively transmit the load or stress to the filler when filler is added to a polymer.[20] It is also believed that the improvement in stiffness of the nanocomposites was due to the high aspect ratio of platelet structure, since it increased the contact surface between the silicate layers and the polymer, thus increasing the interaction between them.[16,18] This high aspect ratio of MMT increased the tensile and flexural modulus of the nanocomposites by increasing the nanofiller contact surface with the PP/ABS matrix. In addition, the degree of exfoliation or intercalation of the clay, which is one of the factors contributing to the improvement of mechanical properties, is proportional to an increase of modulus of nanocomposites. The degree of exfoliation depends on the compatibility between clay and polymer.[18] The degree of intercalation and the interlayer distance between the silicate layers are investigated further in the morphology section.

It is apparent that PP/ABS blend containing no PP-g-MA exhibits better fracture resistance than the compatibilized PP/ABS blend and nanocomposites. This implies that a strong interfacial bonding between PP and ABS, due to PP-g-MA, is detrimental to the impact toughness of the blend and nanocomposites, since the strong interfacial bonding may lead to substantial reduction in debonding and cavitation of the particles from the matrix PP/ABS blend and nanocomposites, leading to lower fracture toughness.[21]

According to Hasegawa et al., both of the maleated PP and clays are responsible for the reduction of the impact strength and elongation at break of PP/PP-g-MA/clay nanocomposites.[1] With the presence of maleic anhydride content, the free radical maleic anhydride grafting process is accompanied by the chain scission and low molecular mass of the corresponding PP-g-MA, thus affecting the impact performances of the nanocomposites.[4] Another possibility is probably due to the MMT particles which hindered the local chain motions of the polymer molecules that enable them to shear yield, which can sharply decrease the impact resistance of the materials.[22] Incomplete dispersion of nanoparticles in the nanocomposites may also contribute to the poor impact performance, which forms aggregates that cause premature crack formation, leading to embrittlement.[23]

Morphological properties

Scanning electron microscopy. SEM was used to investigate the state of dispersion and the particle size of ABS in PP/ABS blends. The test was examined based on the fracture surfaces of the notched Izod impact test samples, which was conducted at room temperature. The samples were etched with THF for 24 h to remove or to dissolve out the ABS dispersed phase in PP continuous phase. The empty spaces or the black holes left behind in the morphological images indicate the ABS phase, as shown in Figure 6. Figure 6(a) shows the morphology of uncompatibilized PP/ABS blend, while Figure 6(b) shows the morphology of compatibilized PP/ABS with PP-g-MA, respectively, at a magnification of 250. Compatibilization effects are most clearly indicated by comparing the fracture surface of blends containing 4 phr of PP-g-MA.

As expected, blends containing no compatibilizer exhibited coarse and heterogenous phase dispersions, while compatibilized blends showed a finer and more homogeneous dispersion of ABS particles in PP matrix. The droplets of ABS particles in PP/ABS blends are spherical, with the mean diameter of the dispersed particles approximately 10.7 μm. The average particle size diameter was decreased to 5.54 μm upon the addition of 4 phr of PP-g-MA in PP/ABS blends. The substantial reduction in particle size indicates an increase in the compatibility between ABS and PP. In the presence of PP-g-MA, the interfacial adhesion between these polymers was improved, subsequently reducing the interfacial tension between PP and ABS. This was due to the dipole–dipole interactions or dipolar interactions produced from the interaction between the polar maleic anhydride group of PP-g-MA and the polar nitrile group of ABS. The schematic reaction between ABS and PP-g-MA was shown earlier in Figure 4. According to George et al., the size of the dispersed nitrile rubber (NBR) domains decreased with the addition of maleic anhydride modified PP, which is caused by the dipolar interactions between maleic anhydride and NBR polar group.[14] Similar findings have also been observed by Lee et al. who also studied PP/ABS blends with the use of a compatibilizer. Conclusively, the size of the dispersed phase decreased in the presence of PP-gMA which acts as a compatibilizer in PP/ABS blends.[5]

X-ray diffraction. Figure 7 shows the X-ray diffraction (XRD) pattern over the 2θ range from 2° to 10°, while Table 2 presents a summary of the XRD results calculated from the

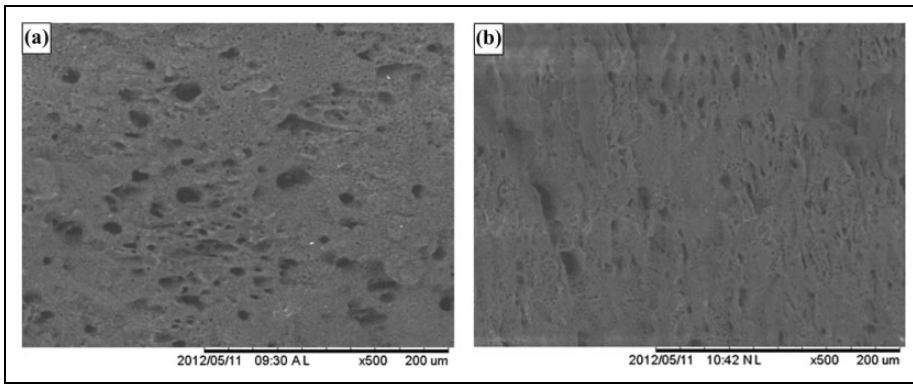

Figure 6. Scanning electron micrographs of fracture surfaces of PP/ABS blends (a) 60/40 PP/ABS blend (b) 60/40 PP/ABS blend with 4 phr PP-g-MA. PP: polypropylene; PP-g-MA: polypropylene-grafted maleic anhydride; ABS: acrylonitrile–butadiene–styrene.

(001) plane peaks for all of PP/ABS nanocomposites. From Figure 7, the characteristic peak (001) of neat MMT was observed at about $2\theta = 3.45^\circ$, which corresponded to a *d*-spacing of 2.56 nm. PP/ABS blend did not show any peaks in XRD analysis and therefore were used as a baseline to prove the existence of diffraction peaks resulting from the dispersed MMT in the polymer matrix. When PP/ABS blend was incorporated with 3 phr MMT (P60M3), the diffraction peaks were slightly shifted toward a lower angle, from $2\theta = 3.45^\circ$ to $2\theta = 2.69^\circ$. Thus implies that the interlayer distance increased from 2.56 to 3.29 nm during the melt blending process. This clearly indicates that the macromolecular chains had intercalated into the galleries of clay. According to As'habi et al. in a study on PA6/ABS/clay nanocomposites, intercalated structure was formed since the *d*-spacing was increased, which indicated that some ABS molecular chains were intercalated between the clay galleries.[24] The increment in the interlayer spacing of MMT is evidence that PP and ABS polymer chains were intercalated in between the gallery of MMT. The increment of interlayer spacing for MMT may be due to the organic modification of MMT. The organic surfactant increased the intergallery distance and reduced the electrostatic attraction between the adjacent platelets providing the possibility for PP and ABS chains to diffuse between the MMT layers during processing.[25]

However, the interlayer spacing of MMT in PP/ABS blend decreased slightly from 3.29 to 3.26 nm, as the MMT content increased from 3 to 5 phr, respectively. This could be attributed to the filler–filler interaction of the clay at high filler loadings, hence resulting in agglomerates, and thus intercalation of the polymer melt into interlayer clays became more difficult.[3,16] This finding is consistent with the previous study.[3,6,26] The increased intensity of the (001) peaks at 5 phr MMT seen in Figure 7 indicates that MMT tends to agglomerate or flocculate with increasing concentration of MMT. Jiang et al. also observed an increase in the intensity at 5 wt% of MMT and larger agglomeration with higher MMT content.[26]

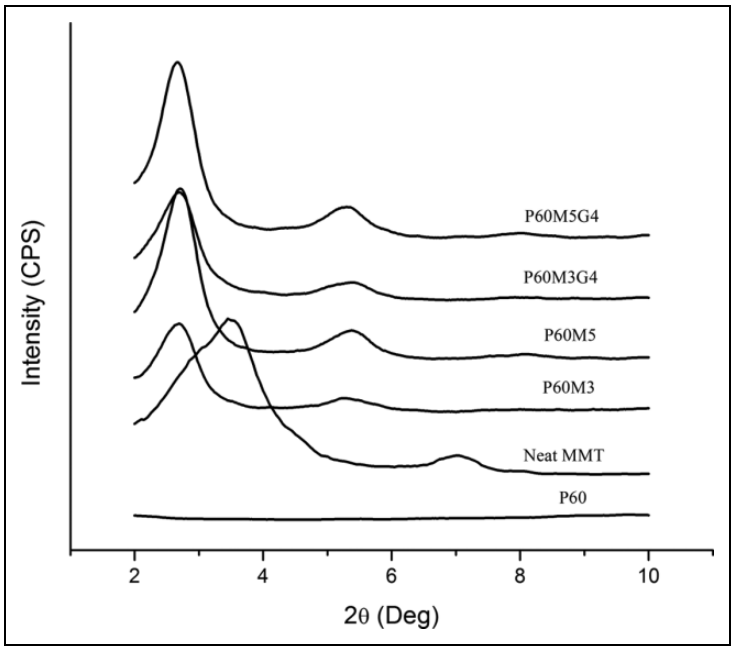

Figure 7. XRD pattern of PP/ABS nanocomposites. PP: polypropylene; ABS: acrylonitrile–butadiene–styrene; XRD: X-ray diffraction.

Table 2. Summary of XRD analysis of PP/ABS nanocomposites.

Designation	PP (wt%)	ABS (wt%)	MMT (phr)	PP-g-MA (phr)	2θ	*d*-spacing (nm)
P60	60	40	–	–	–	–
MMT	–	–	100	–	3.45	2.56
P60M3	60	40	3	–	2.69	3.29
P60M3G4	60	40	3	4	2.69	3.29
P60M5	60	40	5	–	2.71	3.26
P60M5G4	60	40	5	4	2.67	3.31

PP: polypropylene; PP-g-MA: polypropylene-grafted maleic anhydride; ABS: acrylonitrile–butadiene–styrene; MMT: montmorillonite; XRD: X-ray diffraction.

Figure 7 also shows the effect of the incorporation of PP-g-MA compatibilizer on the XRD patterns of PP/ABS nanocomposites containing 3 and 5 phr of MMT. Apparently, when PP-g-MA at 4 phr was employed, a slight improvement in the increment of interlayer was observed for PP/ABS nanocomposite containing 5 phr of MMT, as indicated by the diffractograms. The peaks for PP/ABS nanocomposites at 5 phr of MMT were shifted from $2\theta = 2.71^\circ$ to a lower angle, $2\theta = 2.67^\circ$, upon incorporation of 4 phr PP-g-MA, implying that the *d*-spacing was increased from 3.26 to 3.31 nm, respectively.

This result indicated that PP-g-MA would contribute to a better intercalation effect in PP/ABS nanocomposites. Blending of PP and ABS with only MMT certainly does not increase the degree of intercalation because PP is nonpolar in structure and is not reactive toward clay surfaces. However, by introducing into the system a polar functional group that was reactive toward the polymer matrix and clay surface, in this case is PP-g-MA, a higher degree of intercalation could be obtained. This improvement in the degree of intercalation is due to the strong interaction between the polar PP-g-MA molecules and the silicate layers, where the driving forces for intercalation originate from the strong hydrogen bonding between the maleic anhydride groups and the octadecylamine groups of the silicates, as proposed earlier in Figure 5. This result was consistent with the results obtained in the mechanical properties section which showed an increment in modulus of the nanocomposites.

Transmission electron microscopy. Transmission electron microscopic (TEM) analysis was also conducted to further investigate the dispersion of the PP/ABS nanocomposites, as shown in Figure 8 reporting PP/ABS nanocomposites with and without compatibilizer at various MMT content. Figure 8(a) and (c) revealed the PP/ABS nanocomposites at 3 phr of MMT without and with the addition of PP-g-MA content of 4 phr, respectively. While Figure 8(b) and (d) show the respective nanocomposites at 5 phr of MMT without and with 4 phr of PP-g-MA. Based on Figure 8(a), stacked silicate platelets observed in P60M3 indicated that the MMT existed in the sample. The MMT platelet seems to be skewed or tilted a little and agglomerated at low concentration of MMT but shows better alignment at higher concentration of MMT. The addition of 3 phr of MMT in PP/ABS blend clearly showed that it has increased the interlayer distance in XRD analysis, thus improved the mechanical properties of the sample, as discussed in previous section of this study.

Figure 8(b) shows the TEM image of uncompatibilized PP/ABS nanocomposites containing 5 phr of MMT. The MMT layers of P60M5 seem to have a better alignment in comparison with the alignment of silicate platelets in P60M3. When 5 phr of MMT was added in PP/ABS blend, better dispersion of the clay was obtained. It can be observed from XRD measurement earlier that the intergallery spacing of MMT slightly decreased, as the (001) peak shifted to higher angle due to the agglomeration of MMT platelets. From Figure 8(b), the dark lines are the stacks of MMT layers and some of the stacks consisted of more platelets, appeared to be darker and thicker indicating that agglomeration of MMT has occurred. This results in decrement of intergallery spacing of MMT, as had been discussed in XRD section previously.

Previous study by Balakrishnan et al. showed a similar agglomeration of MMT in PLA/LLDPE nanocomposites.[25] It was discovered that at higher MMT concentration, more agglomerates of MMT were visible in the nanocomposites due to the filler–filler interactions of MMT. These interactions results in agglomeration which restricted delamination of MMT and eventually reduced the exfoliation degree. The agglomerations had acted as a stress concentrator leading to poor mechanical properties in terms of tensile, flexural, and impact strength.

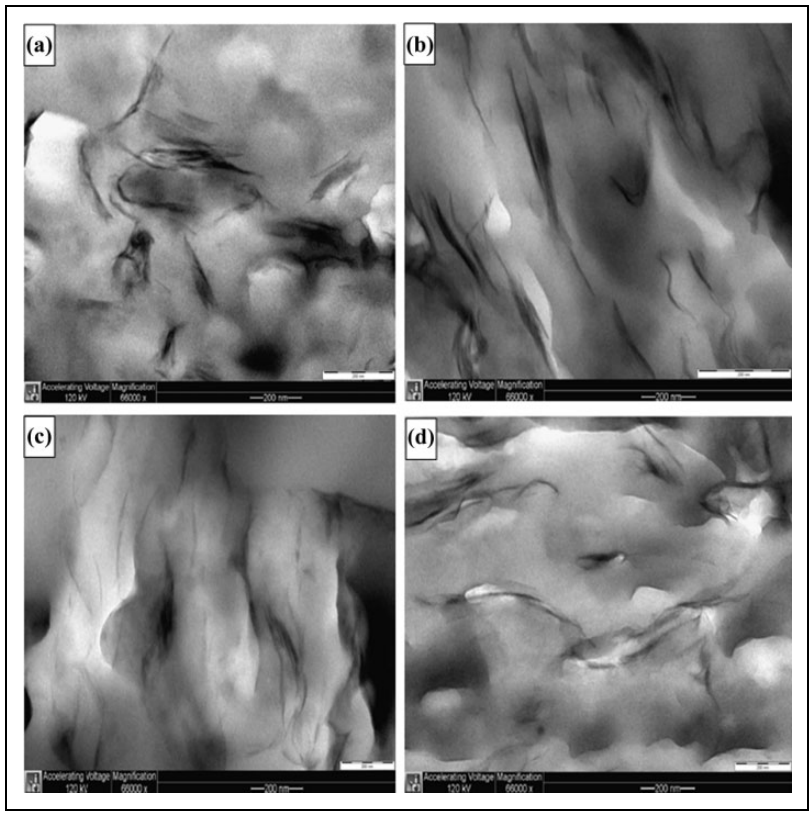

Figure 8. TEM micrographs of PP/ABS nanocomposites (a) P60M3, (b) P60M5, (c) P60M3G4, and (d) P60M5G4.

Figure 8(c) and (d) shows the TEM images of compatibilized PP/ABS nanocomposites with PP-g-MA. Interestingly, the compatibilizing efficiency of the PP-g-MA in PP/ABS nanocomposites was seemingly slightly better than that of the uncompatibilized PP/ABS nanocomposites (Figure 8(a) and (c)) in terms of the agglomerates and the dispersion of MMT layers. Both of Figure 8(c) and (d) presents the intercalated structure of MMT layers. The stacks of MMT became finer and less thick compared to uncompatibilized nanocomposites. Moreover, it is also possible to observe good clay dispersion together with tactoids for compatibilized nanocomposites containing 3 phr of MMT. Recall that the intergallery spacing of MMT in P60M3 and P60M3G4 did not have any significant changes in XRD measurement. However, since TEM micrographs showed the finely dispersed silicate layers and the less aggregation of MMT, it proved that the intercalation has occurred in the nanocomposite. Basically, for sample P60M5 and P60M5G4, results of TEM analysis were in line and consistent with the results obtained from XRD analysis.

Conclusion

In this study, the effects of the addition of 4 phr PP-g-MA compatibilizer and MMT content on the mechanical properties and morphology of the PP/ABS blend and its nanocomposites were investigated. The tensile and flexural modulus of PP/ABS blend and nanocomposites containing 3 and 5 phr MMT increased remarkably, as PP-g-MA was added to the PP/ABS blend and nanocomposites. A significant increase was also observed in tensile and flexural strength of PP/ABS blend and nanocomposites upon incorporation of 4 phr PP-g-MA, however, the impact strength showed a slight decrease with the addition of PP-g-MA and MMT. As the MMT content was increased from 3 to 5 phr, the modulus was observed to increase. However, there was a slight decrease in the strength of the blend and nanocomposites. Morphological studies showed that the dispersed particle size was significantly reduced in the blend, as the blend was compatibilized with PP-g-MA, which could explain the improvement in mechanical strength. XRD showed an increment in the intergallery spacing upon incorporation of MMT. However, further improvement in this spacing was observed with the addition of 4 phr of PP-g-MA. From the TEM micrographs, the MMT layers were mostly located in the interface and intercalated structures were found in the PP/ABS nanocomposites. TEM micrographs showed the finely dispersed silicate layers and the reduced agglomeration of MMT upon addition of 4 phr of PP-g-MA.

Acknowledgements

This research was supported by a grant (Vot. No. 4F060) from the Ministry of Higher Education (MOHE) Malaysia. The authors would like to thank the Research Management Centre (RMC) and Material and Manufacturing Research Alliance (MMRA).

Declaration of conflicting interests

The author(s) declared no potential conflicts of interest with respect to the research, authorship, and/or publication of this article.

Funding

The author(s) received no financial support for the research, authorship, and/or publication of this article.

References

1. Hasegawa N, Kawasumi M, Kato M, et al. Preparation and mechanical properties of polypropylene-clay hybrids using a maleic anhydride-modified polypropylene oligomer. *J Appl Polym Sci* 1998; 67: 87–92.
2. Kato M, Usuki A, and Okada A. Synthesis of polypropylene oligomer—cclay intercalation compounds. *J Appl Polym Sci* 1997; 66: 1781–1785.
3. Lai SM, Chen WC, and Zhu XS. Melt mixed compatibilized polypropylene/clay nanocomposites. II. Dispersion vs. Thermal properties, optical transmittance, and fracture behaviors. *J Compos Mater* 2011; 45(25): 2613–2631.

4. Reichert P, Nitz H, Klinke S, et al. Poly(propylene)/organoclay nanocomposite formation: influence of compatibilizer functionality and organoclay modification. *Macromol Mater Eng* 2000; 275: 8–17.
5. Lee H, Sung YT, Lee Y, et al. Effects of PPgMAH on the mechanical, morphological and rheological properties of polypropylene and poly(acrylonitrile-butadiene-styrene) blends. *Macromol Res* 2009; 17: 417–423.
6. Kim HS, Park BH, Choi JH, et al. Preparation and mechanical properties of acrylonitrile-butadiene-styrene copolymer/clay nanocomposites. *J Appl Polym Sci* 2008; 107: 2539–2544.
7. Patel AC, Brahmbhatt RB, Sarawade BD, et al. Morphological and mechanical properties of pp/abs blends compatibilized with PP-g-acrylic acid. *J Appl Polym Sci* 2001; 81: 1731–1741.
8. Kum C, Sung YT, Kim Y, et al. Effects of compatibilizer on mechanical, morphological, and rheological properties of polypropylene/poly(acrylonitrile-butadiene-styrene) blends. *Macromol Re*s 2007; 15: 308–314.
9. Sung YT, Kim YS, Lee YK, et al. Effects of clay on the morphology of poly(acrylonitrile-butadiene-styrene) and polypropylene nanocomposites. *Polym Eng Sci* 2007; 4: 1671–1677.
10. Kim DH, Fasulo PD, Rodgers WR, et al. Structure and properties of polypropylene-based nanocomposites: effect of PP-g-MA to organoclay ratio. *Polymer* 2007; 48: 5308–5323.
11. Lai SM, Chen WC, and Zhu XS. Melt mixed compatibilized polypropylene/clay nanocomposites: part 1 – the effect of compatibilizers on optical transmittance and mechanical properties. *Compos A* 2009; 40: 754–765.
12. Nam B and Son Y. Evaluations of PP-g-GMA and PP-g-HEMA as a compatibilizer for polypropylene/clay nanocomposites. *Polym Bull* 2010; 65: 837–847.
13. Ding C, Jia D, He H, et al. How organo-montmorillonite truly affects the structure and properties of polypropylene. *Polym Test* 2005; 24: 94–100.
14. George S, Varughese KT, and Thomas S. Thermal and crystallisation behaviour of isotactic polypropylene/nitrile rubber blends. *Polymer* 2000; 41: 5485–5503.
15. Hoon KD, Fasulo PD, Rodgers WR, et al. Effect of the ratio of maleated polypropylene to organoclay on the structure and properties of TPO-based nanocomposites. Part I: morphology and mechanical properties. *Polymer* 2007; 48: 5960–5978.
16. Lim JW, Hassan A, Rahmat AR, et al. Morphology, thermal and mechanical behavior of polypropylene nanocomposites toughened with poly(ethylene-co-octene). *Polym Int* 2006; 55: 204–215.
17. Kim HS, Lee BH, Choi SW, et al. The effect of types of maleic anhydride-grafted polypropylene (mapp) onthe iinterfacial adhesion properties of bio-flour-filled polypropylene composites. *Compos A* 2007; 38: 1473–1482.
18. Kornmann X, Lindberg H, and Berglund LA. Synthesis of epoxy–clay nanocomposites. Influence of the nature of the curing agent on structure. *Polymer* 2001; 42: 4493–4499.
19. Chow WS, Ishak MZA, Karger-Kocsis J, et al. Compatibilizing effect of maleated polypropylene on the mechanical properties and morphology of injection molded polyamide 6/polypropylene/organoclay nanocomposites. *Polymer* 2003; 44: 7427–7440.
20. Pavlidou S and Papaspyride CD. A review on polymer–layered silicate nanocomposites. *Prog Polym Sci* 2008; 33: 1119–1198.
21. Tjong SC, Xu SA, Li RKY, et al. Mechanical behavior and fracture toughness evaluation of maleic anhydride compatibilized short glass fiber/SEBS/polypropylene hybrid composites. *Compos Sci Technol* 2002; 62: 831–840.
22. Stevenson JC.Impact modifiers: Providing a boost to impact performance. *J Vinyl Technol* 1995; 1: 41–45.

23. Gam KT, Miyamoto M, Nishimura R, et al. Fracture behavior of core-shell rubber–modified clay-epoxy nanocomposites. *Polym Eng Sci* 2003; 43: 1635–1645.
24. As'habi L, Jafari S, Khonakdar H, et al. Morphological, rheological and thermal studies in melt processed compatibilized PA6/ABS/clay nanocomposites. *J Polym Res* 2011; 18: 197–205.
25. Balakrishnan H, Hassan A, Wahit MU, et al. Novel toughened polylactic acid nanocomposite: mechanical, thermal and morphological properties. *Mater Des* 2010; 31(7): 3289–3298.
26. Jiang L, Zhang J, and Wolcott MP. Comparison of polylactide/nano-sized calcium carbonate and polylactide/montmorillonite composites: reinforcing effects and toughening mechanisms. *Polymer* 2007; 48: 7632–7644.